Journal of Invertebrate Pathology 114 (2013) 11–21

Contents lists available at SciVerse ScienceDirect

Journal of Invertebrate Pathology

journal homepage: www.elsevier.com/locate/jip

Description and phylogeny of *Zelenkaia trichopterae* gen. et sp. nov. (Microsporidia), an aquatic microsporidian parasite of caddisflies (Trichoptera) forming spore doublets

Miroslav Hyliš [a,*], Miroslav Oborník [b,c], Jana Nebesářová [a,b,c], Jiří Vávra [b,c]

[a] Laboratory of Electron Microscopy, Faculty of Science, Charles University, Prague, Czech Republic
[b] Biology Centre, Institute of Parasitology, Czech Academy of Sciences, České Budějovice, Czech Republic
[c] University of South Bohemia, Faculty of Science, České Budějovice, Czech Republic

ARTICLE INFO

Article history:
Received 31 January 2012
Accepted 23 April 2013
Available online 8 May 2013

Keywords:
Microsporidia
Zelenkaia trichopterae gen. et sp. n.
Trichoptera
Amphipoda
rDNA phylogeny
Ultrastructure

ABSTRACT

Two novel microsporidia infecting the fat body tissues in larvae of two hosts, *Halesus digitatus* and *Micropterna sequax* (Trichoptera, Limnephilidae), were investigated using light and electron microscopy and rDNA sequence analyses. The molecular and morphological characters of these isolates warrant creation of a new microsporidian genus, *Zelenkaia* gen. n., with two species, one named herein. Developmental stages of *Zelenkaia* spp. have single nuclei. In sporogony, a plasmodium with four nuclei gives rise by rosette-like budding to two pairs of uninucleate sporoblasts, each within a thin-walled, subpersistent sporophorous vesicle. Sporoblasts and mature spores adhere temporary together, forming doublets oriented in parallel, within the sporophorous vesicle. Spores are long-oval and uninucleate, and those of the type species *Z. trichopterae* measure 10.3 × 3.5 μm and have 24–25 polar filament coils. Phylogenetic analysis based on rDNA places *Zelenkaia* spp. within the aquatic clade of microsporidia and, more specifically, in the clade containing some microporidia from amphipod hosts.

1. Introduction

With more than 1300 described species in 172 genera, microsporidia are very common parasitic organisms (Cali and Takvorian, 2011). They are almost exclusively parasites of animals, with crustaceans and insects being their most frequent hosts. Many microsporidia, primarily those infecting terrestrial hosts, are transmitted among susceptible conspecific hosts by ingestion of infective spores.

It is of fundamental interest, however, that some microsporidian species, uniquely from aquatic invertebrates such as crustaceans and insects, have spores that are not orally infective for conspecific hosts (Vávra, 1964b; Vávra and Larsson, 1994; Vávra et al., 2005; Hyliš et al., 2007; Wolinska et al., 2011).

Microsporidia, parasitizing caddisflies are of special interest to the study of the evolution of the Phylum Microsporidia for several reasons. (1) Trichopteran lifecycles include aquatic (larval) and terrestrial (imaginal) stages. (2) Trichopteran larvae harbor microsporidia that produce mature spores that are not infective for the original host (Heilveil et al., 2001; Hyliš et al., 2007). (3) Phylogenetically, microsporidia from trichopteran hosts are related to the Amblyosporidae clade, many representatives of which have two-host lifecycles (Vossbrinck et al., 2004; Becnel et al., 2005; Andreadis, 2005, 2012). These observations support the assumption that some extinct or extant trichopteran microsporidia may also require an intermediate host to complete their life cycle. In addition, the order Trichoptera is closely related to Lepidoptera, an insect order hosting many genera and species of Microsporidia. So studies on trichopteran parasites might shed light on the origin and diversification of terrestrial microsporidia groups.

Representatives of 10 microsporidian genera and 24 species have been identified in Trichoptera (Larsson, 1995; Canning and Vávra, 2000; Hyliš et al., 2007). This paper describes the morphology and molecular phylogeny of two species of caddisfly microsporidia that possess unique structural characters and represent a new genus.

2. Materials and methods

2.1. Origin of isolates

Two microsporidian isolates with morphologically similar mature spores, designated as isolates iMS1 and iMS2, were discovered infecting trichopteran larvae in Bulgaria in June 2001. iMS1 was found in one living larva of *Halesus digitatus* Schrank, 1781 (Trichoptera, Limnephilidae) in a small temporary stream near the village Levishte, Bulgaria (43°07′59.14″ North; 23°46′04.62″ East).

* Corresponding author. Address: Laboratory of Electron Microscopy, Faculty of Science, Charles University, Viničná 7, 128 44 Prague 2, Czech Republic.
E-mail address: mirekhylis@volny.cz (M. Hyliš).

0022-2011/$ - see front matter © 2013 Elsevier Inc. All rights reserved.
http://dx.doi.org/10.1016/j.jip.2013.04.010

iMS2 was found in several dead larvae of *Micropterna sequax* McLachlan, 1875 (Trichoptera, Limnephilidae) in a small pond near the village Dragichevo, Bulgaria (42°38′28″ North; 23°09′0.58″ East).

2.2. Examination of infected host tissues: scanning and transmission electron microscopy

Fresh host tissues infected with iMS1, a suspension of necrotic and lysed tissues with iMS2, and tissue smears of both organisms stained with Giemsa (Sigma® Diagnostic Accustain) were examined under light microscopy. Spores were immobilized using the agar method (Vávra, 1964a) and were measured ($n = 50$) with an Image Splitting Eyepiece (Vickers Instruments Ltd.) (Vávra and Maddox, 1976). For field emission scanning electron microscopy (FESEM), an aqueous suspension of fresh purified spores of iMS1 was rapidly frozen in liquid nitrogen, and then was examined in a non-coated state in a JEOL JSM-7401F scanning electron microscope. For transmission electron microscopy (TEM), iMS1 infected adipose tissues were fixed for 24 h in 2.5% glutaraldehyde in 0.1 M cacodylate buffer (pH 7.2) and postfixed in 2% OsO_4 in the same buffer. Fixed tissue was dehydrated through an ascending ethanol and acetone series and embedded in Araldite – Poly/Bed® 812 mixture. Thin sections were cut on a Reichert–Jung Ultracut E ultramicrotome and stained using uranyl acetate and lead citrate. Sections were examined and photographed using a JEOL JEM-1011 electron microscope. Fine structure measurements were performed using a Megaview III camera and analySIS 3.2 software (Soft Imaging System®).

2.3. rDNA sequences; phylogenetic analysis

DNA was isolated from fresh purified spores of iMS1 and iMS2 according to the protocol of Hyliš et al. (2005). Primers ss530f: ls580r (Weiss and Vossbrinck, 1999) were used to amplify the small subunit (in part), ITS region, and large subunit rDNA (in part). The PCR reaction (95 °C for 2 min; 30 cycles of 94 °C for 1 min, 50 °C for 1 min, 72 °C for 2 min; and 72 °C for 10 min) was conducted in a total volume of 25 μl with 50–100 ng of DNA, 25 pmol of each primer, 1 unit Taq polymerase (TAKARA BIO INC. Otsu, Shiga, Japan) and buffer/dNTP (TaKaRa) according to manufacturers instructions. PCR products were separated using 1% agarose gel electrophoresis, extracted from the gel, purified using the DNeasy Tissue Kit® (QIAGEN, Germantown, Maryland, USA), cloned (TOPO TA Cloning Kits®, Invitrogen, Carlsbad, California, USA) and sequenced on an automatic sequencer (Beckman CEQ 2000 XL). The sequences were aligned using the ClustalX program (Thompson et al., 1997), gaps and ambiguously aligned regions were omitted from further analyses.

Analysis was carried out using distance, maximum parsimony and maximum likelihood methods. The distance matrix was calculated using the LogDet paralinear model with the portion of invariable sites included as estimated in the maximum likelihood search. Maximum Parsimony (MP) trees were constructed using PAUP 4b10 (Swofford, 2000) with TBR as a branch-swapping method and 1000 bootstrap replicates. Maximum likelihood trees were constructed by PHYML program (Guindon and Gascuel, 2003), using the GTR model for nucleotide substitutions with discrete gamma distribution in 4 + 1 categories; all parameters (gamma shape, proportion of invariants) were estimated from the dataset. Multiple datasets for ML bootstrap analyses were prepared using SeqBoot (PHYLIP 3.6.3; Felsenstein, 2001). ML bootstrap support was computed in 300 or 1000 replicates using PHYML program with the TN93 model for nucleotide substitutions and one category of sites with a TI/TV ratio estimated from the data set.

Table 1
Species list of microsporidian SSU rDNA sequences included in the phylogenetic analysis, hosts from which they were obtained, taxonomic classification of hosts and GenBank accession numbers.

Organism	Host	Host taxonomic classification	GenBank Acc. No.
Amblyospora bracteata	*Odagamia ornata*	Insecta, Diptera, Simuliidae	AY090068
Amblyospora ferocious	*Psorophora ferox*	Insecta, Diptera, Culicidae	AY090062
Berwaldia schaefernai	*Daphnia galeata*	Crustacea, Cladocera, Daphniidae	AY090042
Episeptum circumscriptum	*Hydropsyche incognita*, *H. siltalai*	Insecta, Trichoptera, Hydropsychidae	DQ864440
Episeptum pseudoinversum	*Sericostoma personatum*	Insecta, Trichoptera, Sericostomatidae	DQ864441
Episeptum trichoinvadens	*Potamophylax cingulatus*	Insecta, Trichoptera, Limnephilidae	DQ864439
Gurleya daphniae	*Daphnia pulex*	Crustacea, Cladocera, Daphniidae	AF439320
Gurleya vavrai	*Daphnia longispina*, *D. pulex*	Crustacea, Cladocera, Daphniidae	AF394526
Hazardia milleri	*Culex quinquefasciatus*	Insecta, Diptera, Culicidae	AY090067
Hazardia sp.	*Anopheles crucians*	Insecta, Diptera, Culicidae	AY090066
Larssonia obtusa	*Daphnia pulex*	Crustacea, Cladocera, Daphniidae	AF394527
Marssoniella elegans	*Cyclops vicinus*	Crustacea, Copepoda, Cyclopidae	AY090041
Microsporidium sp. Angskar 21	*Daphnia longispina*	Crustacea, Cladocera, Daphniidae	EU075350
Microsporidium sp. BKES1 CAL	*Odontogammarus calcaratus*	Crustacea, Amphipoda, Eulimnogammaridae	FJ756018
Microsporidium sp. BKES1 KES	*Pallaseopsis kessleri*	Crustacea, Amphipoda, Pallaseidae	FJ756019
Microsporidium sp. BKES1 LAT	*Brandtia latissima latior*	Crustacea, Amphipoda, Acanthogammaridae	FJ756020
Microsporidium sp. BLAP2	*Acanthogammarus lappaceus*	Crustacea, Amphipoda, Acanthogammaridae	FJ756026
Microsporidium sp. BLAT20	Brandtia latissima lata	Crustacea, Amphipoda, Acanthogammaridae	FJ756071
Microsporidium sp. BSEI1 LAC	*Gammarus lacustris*	Crustacea, Amphipoda, Gammaridae	FJ756154
Microsporidium sp. CRANA	*Crangonyx* sp.	Crustacea, Amphipoda, Crangonyctidae	AJ966721
Microsporidium sp. MIC1	*Daphnia galeata*	Crustacea, Cladocera, Daphniidae	FJ794862
Microsporidium sp. Ripley Pond I	*Daphnia pulicaria*	Crustacea, Cladocera, Daphniidae	EU075355
Microsporidium sp. Turtle Lake	*Daphnia pulicaria*	Crustacea, Cladocera, Daphniidae	EU075357
Octosporea muscaedomesticae	*Musca domestica*, *Phormia regina*	Insecta, Diptera, Muscidae/Calliphoridae	FN794114
Paraepiseptum plectrocnemiae	*Plectrocnemia conspersa*	Insecta, Trichoptera, Polycentropodidae	DQ864438
Paraepiseptum polycentropi	*Hydropsyche fulvipes*, *Polycentropus flavomaculatus*	Insecta, Trichoptera, Hydropsychidae/Polycentropodidae	DQ864437
Parathelohania anophelis	*Anopheles quadrimaculatus*	Insecta, Diptera, Culicidae	AF027682
Parathelohania obesa	*Anopheles crucians*	Insecta, Diptera, Culicidae	AY090065
Senoma globulifera	*Anopheles messeae*	Insecta, Diptera, Culicidae	DQ641245
Trichotuzetia guttata	*Cyclops vicinus*	Crustacea, Copepoda, Cyclopidae	AY326268
Vairimorpha sp.	*Solenopsis richteri*	Insecta, Hymenoptera, Formicidae	AF031539
Zelenkaia sp. (=iMS 2)	*Micropterna sequax*	Insecta, Trichoptera, Limnephilidae	EF537881
Zelenkaia trichopterae (=iMS 1)	*Halesus digitatus*	Insecta, Trichoptera, Limnephilidae	EF537879

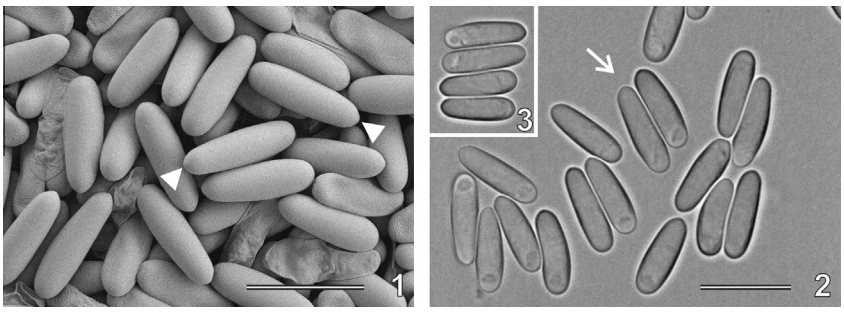

Figs. 1–3. Isolated spores of iMS1 (*Zelenkaia trichopterae*) (Figs. 1 and 2) and iMS2 (*Zelenkaia* sp.) (Fig. 3). Fig. 1. Frozen spores observed with field emission scanning electron microscope. Inconspicuous studs at anterior tips of spores (white arrowheads). Fig. 2. Fresh spores, arranged in doublets, surrounded by inconspicuous sporophorous vesicle (arrow) (light microscope). Fig. 3. Spores of *Zelenkaia* sp. (light microscope). (Bars for Figs. 1–3 = 10 μm.)

The GenBank accession numbers of microsporidian sequences used for phylogenetic analysis are shown in Table 1.

3. Results

3.1. Host and tissue infected

iMS1, isolated from *Halesus digitatus* and iMS2, isolated from *Micropterna sequax*, appeared to be specific to their hosts, each infecting one host species. Of 38 *H. digitatus* larvae examined, only a single larva with a conspicuously white fat body was found to be infected. Microscopic examination confirmed that the infection was restricted to the adipose tissue. Four species of caddisfly larvae representing the trichopteran families Limnephilidae, Philopotamidae and Sericostomatidae were present in the stream, but no infections were found in 30–50 individuals of each species examined.

Several hundred healthy pupae and many dead, decomposing larvae of *M. sequax* were collected at the site where iMS2 was

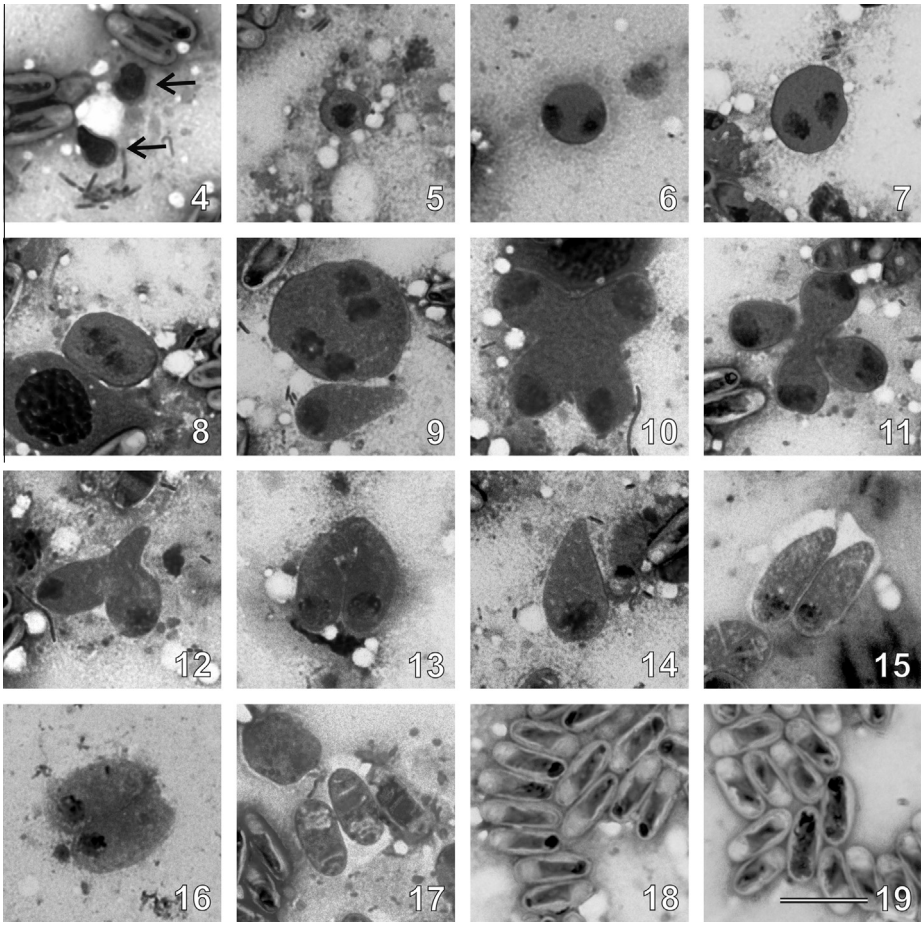

Figs. 4–19. Light micrographs of merogonial (Figs. 4–6) and sporogonial stages and spores (Figs. 7–18) of iMS1 (*Zelenkaia trichopterae*) and spores of iMS2 (*Zelenkaia* sp.) (Fig. 19), Giemsa-stained smears. Fig. 4. Early meronts shortly differentiated from sporoplasms (arrows). Fig. 5. Growing (possibly uninucleate) early meront. Fig. 6. Early meront after first nuclear division. Figs. 7–8. Early sporonts. Fig. 9. Tetranucleate sporonts undergoing nuclear division and transition to sporogonial plasmodium. Figs. 10 and 11. Tetranucleate sporogonial plasmodium budding into rosette-like forms. Figs. 12 and 13. Pairs of uninucleate sporoblasts originated from rosette-like tetranucleate sporogonial plasmodium. Fig. 14. Individual uninucleate sporoblast. Figs. 15–17. Sporoblast doublet in a common sporophorous vesicle (unstained area around spores in Figs. 15 and 17) undergoing sporogenesis. Fig. 18. Mature spores with large, distinctly stained posterosomes at the posterior poles. Fig. 19. Mature and nearly mature spores of *Zelenkaia* sp. (Bar for Figs. 4–19 = 10 μm.)

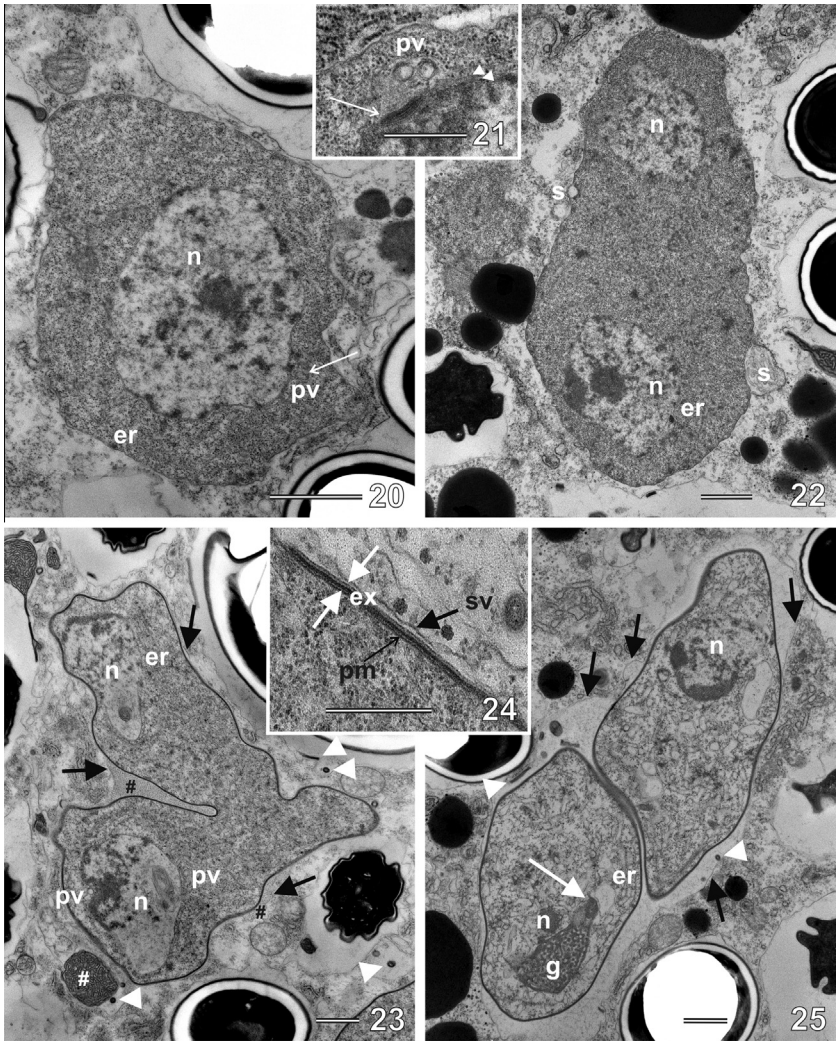

Figs. 20–25. Transmission electron micrographs of merogonial (Figs. 20–22) and sporogonial (Figs. 23–25) stages of iMS1 (*Zelenkaia trichopterae*). Fig. 20. Early uninucleate meront. Nucleus (n); endoplasmic reticulum (er); polar vesicles (pv). Fig. 21. Detailed view of the spindle plaque (white arrow) lying in the depression of the nuclear double membrane (white arrowheads), and of adjacent polar vesicles (pv). Fig. 22. Late binucleate meront approaching the transition to sporogonial plasmodium. Paramural bodies or scindosomes (s). Fig. 23. Sporogonial plasmodium within a sporophorous vesicle (arrows) filled by fine granular material (black #). Later in sporogony this material forms clusters with periodic structure (white #). Fibers in the episporontal space of the sporophorous vesicle (white arrowheads). Fig. 24. Detailed view of the tetralaminar structure of the exospore (ex = exospore, pm = plasma membrane of sporogonial plasmodium, sv = sporophorous vesicle membrane). Fig. 25. Two young sporoblasts within a common sporophorous vesicle (black arrows) (er = lamellae of endoplasmic reticulum; at white arrow is the tip of polar tube formed by a complex of Golgi vesicles (g); at white arrowheads are fibers of the episporontal space. Abbreviations for Figs. 22, 23 and 25: n = nucleus; er = endoplasmic reticulum; pv = polar vesicles. (Bars 20, 22, 23, 25 = 1 μm; 21, 24 = 0.5 μm.)

found. The pupae were not infected ($n = 20$), but all dead larvae were infected ($n > 30$). One larva was selected for further research. Larvae of two species of unidentified caddisflies of the family Limnephilidae were found at the same locality but were not infected ($n = 40$). Tissue tropism for infected larvae at the iMS2 site was not possible to ascertain due to post-mortem changes. The enormous number of spores observed in dead larvae indicated, however, that fat body was most probably the infected tissue.

3.2. Light microscope observations; developmental cycle

Small persistent pairs of similarly oriented spores inside inconspicuous (nearly invisible) sporophorous vesicles were observed in larval tissues of both host species. Spores of the iMS1 and iMS2 were long-oval in shape with distinct posterior vacuoles (Figs. 1–3, 18, 19), and differed only in size. Spores of iMS1 measured 10.3 × 3.5 μm (9.6–11.2 × 3.3–3.7 μm) ($n = 50$, fresh); spores of iMS2 were smaller, measuring 9.5 × 3.7 μm (9.2–9.7 × 3.5–3.8 μm) ($n = 50$, fresh). Life cycle stages other than spores were observed only in iMS1 and are described below.

The earliest stages observed were small rounded uninucleate meronts (3.5–4.0 μm) with large nuclei occupying most of the cell volume (Fig. 4). Uninucleate and binucleate meronts were 5–10 μm in diameter (Figs. 5 and 6). No obvious diplokaryon-like arrangement of nuclei was observed in binucleate cells. Frequently the two nuclei were located at opposite poles of the cell (Fig. 6). The first sporogonial stages had nuclei located closer to the center of the cell (Figs. 7 and 8). Sporonts grew to 10–15 μm, their nuclei divided and a tetranucleate sporogonial plasmodium was formed (Figs. 9–11). Late tetranucleate sporogonial plasmodia (Fig. 9) were the largest stages of the entire developmental cycle observed (18–23 μm) and gave rise to four-lobed formations by rosette-like budding. The cytoplasm looked more dense and granular (Figs. 10 and 11). Separate pairs of uninucleate sporoblasts (15–16 μm), connected at the base were the next developmental stage (Figs. 12 and 13). In smears these stages were mixed together with

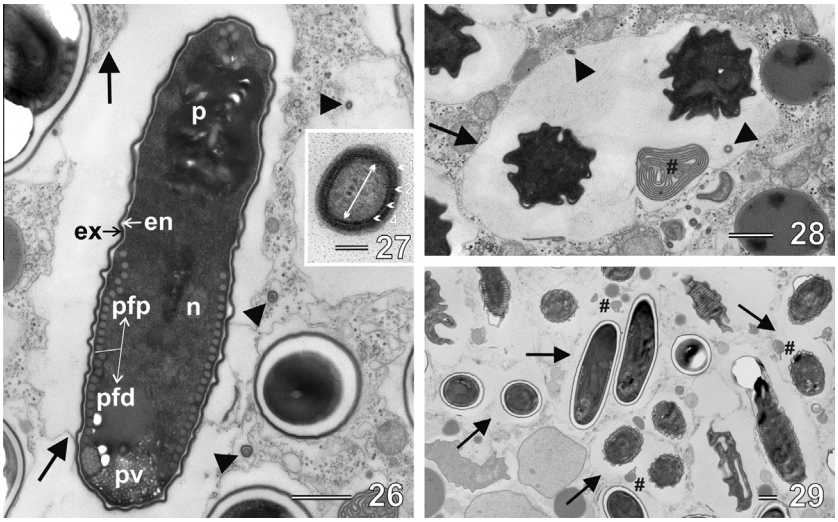

Figs. 26–29. Transmission electron micrographs of late sporogonial stages of iMS1 (=*Zelenkaia trichopterae*). Fig. 26. Late sporoblast/young spore in sporophorous vesicle (arrows). Endospore (en); exospore (ex); proximal (pfp) and distal (pfd) coils of the slightly anisofilar polar filament; posterior vacuole (pv); polaroplast (p); nucleus (n). Fig. 27. Cross section through the fiber in the episporontal space shows electron-dense core surrounded by four layers. Fig. 28. Cross sectioned sporophorous vesicle (arrow) with two sporoblasts. Fibers in the episporal space (arrowheads); helix-like cluster of secretory material (#). Fig. 29. Various stages of late sporogony and sporogenesis are surrounded by SPOV membranes (arrows). Secretory material in the episporontal space of sporophorous vesicle (#). (Bars 26, 28, 29 = 1 μm; 27 = 100 nm).

drop-like uninucleate sporoblasts, evidently artificially breaked-off by smearing (Fig. 14). The final sporogonial stages (14–11 μm) were undergoing sporogenesis accompanied by size reduction (Figs. 15–17). The spores of both isolates had large, distinctly stained posterosomes.

Similar to fresh spores, Giemsa stained spores of iMS1 were slightly longer and narrower than those of iMS2 (Figs. 18 and 19). Stained spores of iMS1 measured 9.7 × 3.3 μm (8.6–10.7 × 2.7–3.5 μm; $n = 50$); those of iMS2 measured 8.9 × 3.6 μm (7.8–9.6 × 2.9–3.7 μm; $n = 50$).

3.3. Scanning and transmission electron microscope observations; ultrastructural characterization

The spore surface of both iMS1 and iMS2 was smooth with an inconspicuous stud at the anterior tip of the spore (Fig. 1). The following ultrastructural data pertain only to the iMS1. Merogonial stages were irregular cells with electron-dense cytoplasm, traces of endoplasmic reticulum, Golgi vesicles and abundant ribosomes. The nucleus occupied a substantial portion of the cell volume; the cytoplasm contained many ribosomes and obscured traces of lamellae of endoplasmic reticulum (Fig. 20). Nucleoli are visible inside nuclei (Figs. 20 and 22). Dividing nuclei in meronts showed spindle plaques lying in a depression of nuclear membrane. Vesicles with double membrane ("polar vesicles") occurred in the vicinity of spindle plaques (Fig. 21). Paramural bodies occurred in merogonial plasmodia when they approached sporogony (Fig. 22). All merogonial stages were in direct contact with the host cell cytoplasm.

Sporogonial stages generally had less electron-dense cytoplasm and more distinct ultrastructure (Figs. 23 and 25). The onset of sporogony was marked by the formation of abundant endoplasmic reticulum, that appeared before the thickening of the plasma membrane by deposition of wall material. Rosette-like budding of sporogonial plasmodia took place simultaneously with the thickening of the plasma membrane and the detachment of the sporophorous vesicle (SPOV) wall from the plasma membrane. The SPOV wall appeared first as a single, very thin, structureless line, closely attached to the border of the sporogonial plasmodium. When the plasmodium began to divide, the SPOV wall lost its adherence to the plasma membrane at the site of the division furrows. Here the fine granular material of the episporontal space appeared (Fig. 23). The tetralaminar structure of the future exospore (Fig. 24) was built on the surface of the budding sporogonial plasmodium by deposition of fine granular secretory material filling the episporontal space of the SPOV (Fig. 23). Later in sporogony, this secretory material formed helical clusters with periodic structure (Figs. 23, 28 and 29). Young sporoblasts existed typically as a pair of cells, temporarily connected by a structureless, electron-dense diffuse material. Each pair was enveloped by a SPOV membrane that formed a loose, somewhat wrinkled sachet forming outpockets into the surrounding host tissue (Figs. 25 and 26). The episporontal secretory material nearly disappeared from the SPOV when the sporoblasts began to mature. At the same time several isolated electron dense thick fibers appeared in the episporontal space (Figs. 25 and 27). In cross sections these fibers showed four layers which surrounded an electron dense core (Fig. 27).

In late sporoblasts and early spores (Fig. 26) the proximal and distal coils of the slightly anisofilar polar filament reached the final number, but the polaroplast, endospore and posterior vacuole were poorly developed. The endospore was of approximately the same thickness as the exospore (Fig. 26). In late sporogenesis the SPOV membrane was thin and wrinkled, loosely ensheathed the spores, and formed deep outpockets into the host cytoplasm (Figs. 26, 28 and 29). A large helix-like cluster of secretory material was present in the episporontal space of each sporophorous vesicle (Fig. 29). The two spores formed inside the common SPOV were similarly oriented, but were independent; the material that had been previously holding them together, now disappeared (Figs. 28 and 29).

The spore wall of a mature spore consisted of plasma membrane, an endospore 180 nm thick and a complex 50 nm exospore composed of at least 10 layers (Figs. 30 and 35). The polar sac-anchoring disk complex was enveloped by an umbrella-like polar sac extending posteriorly to surround the anterior part of the polaroplast (Fig. 33). The polaroplast had two distinct parts: an anterior cup-like part was composed of regularly arranged, closely packed lamellae, while the posterior part consisted of less regularly packed lamellae, arranged perpendicularly to the spore axis (Figs. 30–33). Mature spores had slightly anisofilar polar filaments with 24–26 coils in a single row, consisting of 11–12 thicker distal coils (150 nm; 130–160 nm) and 13–14 thinner proximal coils (130 nm; 120–140 nm) (Fig. 30). Transversal sections of the polar

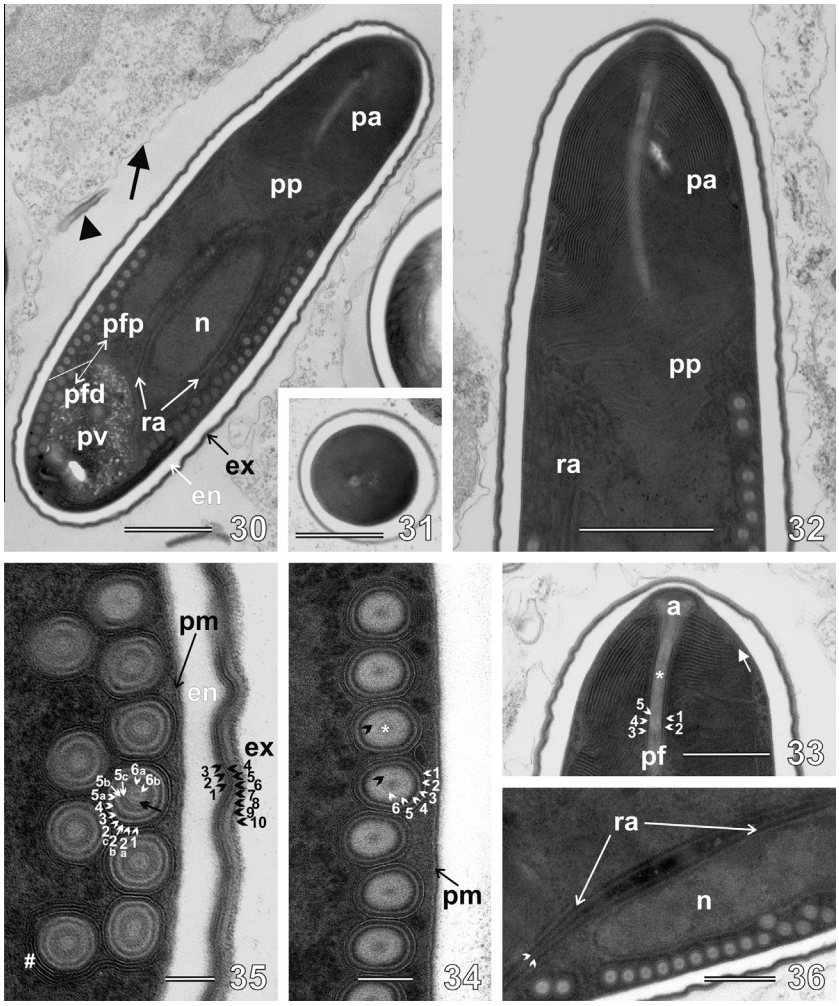

Figs. 30–36. Transmission electron micrographs of spores of iMS1 (=*Zelenkaia trichopterae*). Fig. 30. Mature spore: exospore (ex); endospore (en); posterior vacuole (pv); anterior polaroplast (pa) and posterior polaroplast (pp). Polar filament with thicker distal (pfd) and thinner proximal coils (pfp); endoplasmic reticulum lamellae and polyribosomal agregates (ra); sporophorous vesicle membrane (arrow); fiber of the episporontal space (arrowhead). Fig. 31. Cross sectioned anterior part of the polaroplast. Fig. 32. Longitudinally sectioned apex of the spore showing polaroplast in two distinct parts: anterior cup-like part (pa); posterior part (pp); polyribosomal aggregates (ra). Fig. 33. Longitudinal section through the spore apex showing the polar sac (white arrow) – anchoring disk (a) complex and polar filament (pf). Section reveals its internal organization of five main layers: unit membrane cover layer (1), electron dense layer (2), moderately dense layer (3), second electron dense layer (4), second moderately dense layer (5) and electrondense core (∗). Figs. 34 and 35. Detailed view of the cross sectioned proximal (Fig. 34) and distal (Fig. 35) polar filament coils. Fig. 34. Cross section through anterior polar filaments coils: two layers, 5 and 6, correspond to the layer 5 of the uncoiled part of the polar filament (Fig. 33) (pm = the plasma membrane, ∗ = electrondense core, arrowheads = border of layers 5 and 6). Fig. 35. Cross section displaying the distal polar filament coils with additional sub-layers (2b, 5b, 5c, 6b), and the spore wall. The electron dense cores of polar filament coils are not visible. Fibrillar content of the 6a layer is indicated by arrow, multiple membranous layers of distal coils – by pound sign. Complex exospore (ex) consists of about 10 layers. (en = endospore, pm = plasma membrane). Fig. 36. Lamellae of endoplasmic reticulum (er) and polyribosomes aggregates (ra) surrounding the nucleus (n). (Bars 30, 31, 32 = 1 μm; 33, 36 = 500 nm; 34, 35 = 100 nm.)

filament revealed six layers: a unit membrane-like cover layer (1), electron dense layer (2), moderately dense layer (3), second electron dense layer (4), two moderately dense layers (5) and (6) and an electron-dense core. The general organization of the polar filament was similar along its length. However the thicker distal and thinner proximal coils differed not only in the coil thickness but also in the total number of layers. The proximal coils (Fig. 34) had the same substructure as the straight (“manubrial”) part of the filament (Fig. 33), except the layer 6, which was missing in the straight, manubrial part of the filament. The distal polar filament coils had the most different substructure: the number of polar filament layers increased by insertion of additional sub-layers (2b, 5b, 5c, 6b) (Fig. 35) to the main layers (Fig. 34). The electron-dense core existing in proximal coils (Fig. 34) was missing in distal coils (Fig. 35). The most distal coils were surrounded by multiple membranous layers, probably of endoplasmic reticulum origin. Numerous endoplasmic reticulum lamellae and polyribosomal aggregates were located in the middle part of the spore (Figs. 30 and 36). A large posterior vacuole occupied the posterior pole of the spore.

3.4. Phylogenetic position of iMS1 and iMS2

A band of approximately 1500 bp genomic rDNA was amplified from both isolates with the ss530f: ls580r primers. The partial sequences of ssu rDNA of iMS1 (522 bp; 56.7% GC; GenBank Acc. No. EF537878), of iMS2 (530 bp; 56.1% GC; GenBank Acc. No. EF537880) and the partial sequence of ITS-lsu rDNA of iMS1 (633 bp; 51.7% GC; GenBank Acc. No. EF537879) and iMS2 (670 bp; 52.3% GC; GenBank Acc. No. EF537881) were analyzed separately. The examined sequences of the ssu rDNA were nearly identical for iMS1 and iMS2, they differed only in two nucleotide positions (four, including deletions), while in the ITS-lsu rDNA region they differed in 16 nucleotide positions (21, including

Table 2
Pairwise distances (% nucleotide identity) between taxa based on a partial SSU rRNA gene sequences. Constructed using Geneious® Pro 5.6.3. Microsporidia with maximal similarity with *Zelenkaia* spp. are printed in bold.

	1	2	3	4	5	6	7	8	9	10	11	12	13	14	15	16	17	18	19	20	21	**22**	**23**	**24**	**25**	**26**	27	28	29	30	31	32	33
1 *Microsporidium* sp. Ripley Pond I	100.0																																
2 *Microsporidium* sp. Turtle Lake	99.4	100.0																															
3 *Senoma globulifera*	91.1	91.1	100.0																														
4 *Microsporidium* sp. *Angskar* 21	88.1	88.1	86.4	100.0																													
5 *Larssonia obtusa*	87.8	87.9	86.1	98.5	100.0																												
6 *Berwaldia schaefernai*	92.6	92.6	90.2	99.4	98.4	100.0																											
7 *Gurleya daphniae*	85.0	85.1	84.4	87.2	86.7	90.0	100.0																										
8 *Gurleya vavrai*	84.7	84.8	84.1	87.0	86.8	89.9	99.7	100.0																									
9 *Microsporidium* sp. MIC1	88.3	88.3	87.2	91.1	91.0	93.1	92.1	91.8	100.0																								
10 *Paraepiseptum polycentropi*	84.5	84.0	84.6	86.7	86.5	86.7	81.1	80.9	84.1	100.0																							
11 *Paraepiseptum plectrocnemiae*	84.3	83.7	83.7	86.0	85.5	85.9	81.0	80.8	83.9	94.0	100.0																						
12 *Episeptum circumscriptum*	86.1	85.6	85.5	87.1	86.8	87.1	82.0	81.8	84.4	93.5	93.1	100.0																					
13 *Episeptum pseudoinversum*	87.4	86.9	86.7	88.1	87.7	88.1	82.2	82.0	85.5	92.7	92.1	95.8	100.0																				
14 *Episeptum trichoinvadens*	87.0	86.4	86.4	88.0	87.7	87.8	81.9	81.8	85.6	94.1	94.7	95.8	96.3	100.0																			
15 *Marssoniella elegans*	86.5	86.7	85.9	88.5	88.1	88.8	84.5	84.7	86.9	91.8	90.8	91.3	92.3	92.7	100.0																		
16 *Hazardia milleri*	87.9	88.2	86.7	89.8	89.3	90.1	85.2	85.3	87.4	87.4	87.1	89.3	89.5	89.7	89.6	100.0																	
17 *Hazardia* sp.	86.2	86.5	84.8	88.1	87.8	89.2	83.6	83.9	86.3	86.7	86.7	88.5	88.6	89.0	89.0	95.9	100.0																
18 *Vairimorpha* sp.*S.richteri*	81.1	81.1	80.0	81.3	81.3	81.4	79.2	78.9	81.7	81.2	80.7	81.7	82.1	82.0	81.5	82.0	81.7	100.0															
19 *Microsporidium* sp. BSEI1 LAC	84.8	84.8	84.1	86.2	85.3	86.1	81.9	81.8	86.2	92.5	91.7	93.7	94.0	95.0	89.4	91.1	89.9	84.3	100.0														
20 *Trichotuzetia guttata*	71.3	71.4	71.2	71.2	70.6	71.1	68.1	67.9	70.5	73.0	72.8	72.4	74.3	74.5	71.4	74.0	73.6	68.6	78.8	100.0													
21 *Microsporidium* sp. CRANA	82.3	82.0	80.5	83.2	82.3	83.1	80.1	80.0	82.4	80.7	81.1	82.3	82.6	82.6	80.8	82.4	83.1	78.5	80.9	73.0	100.0												
22 Microsporidium sp. BKES1 LAT	83.8	83.7	81.3	83.7	83.5	83.7	79.9	80.7	84.1	83.7	84.2	85.5	86.0	85.7	84.6	86.7	87.4	80.6	85.4	75.3	80.0	100.0											
23 Microsporidium sp. BKES1 CAL	84.3	84.2	81.9	84.2	84.0	84.2	80.5	81.1	84.6	84.4	84.9	86.1	86.6	86.4	85.0	87.2	87.9	81.1	85.8	75.5	80.5	99.7	100.0										
24 Microsporidium sp. BKES1 KES	83.8	83.7	81.4	83.7	83.5	83.7	80.0	80.6	84.1	83.9	84.4	85.6	86.1	85.9	84.5	86.7	87.2	80.4	85.3	74.7	80.1	98.8	99.1	100.0									
25 Microsporidium sp. BLAT20	84.7	84.6	82.4	84.9	84.5	84.9	80.9	81.5	85.4	83.9	84.4	85.1	86.6	85.9	85.5	86.8	87.6	80.9	85.1	74.3	80.4	96.3	96.6	96.1	100.0								
26 Microsporidium sp. BLAP2	83.8	83.5	82.1	85.7	85.4	85.6	82.0	82.7	84.8	82.5	81.9	82.4	83.2	82.2	85.3	85.9	85.3	80.2	84.0	74.2	78.9	90.6	90.7	90.2	91.0	100.0							
27 *Octosporea muscaedomesticae*	65.3	65.1	64.4	65.2	64.5	65.1	62.9	62.8	65.5	69.2	71.8	70.2	72.1	71.4	65.2	66.6	67.2	63.4	85.2	58.8	80.8	95.5	95.8	95.3	95.0	90.1	100.0						
28 *Parathelohania anophelis*	74.3	74.1	73.8	74.6	74.6	74.4	71.6	72.0	73.3	73.3	72.9	73.7	74.6	74.0	74.5	74.7	74.1	71.4	74.5	62.1	71.8	74.8	75.4	74.8	75.0	75.7	59.4	100.0					
29 *Parathelohania obesa*	74.4	74.1	73.8	74.5	74.5	74.7	71.7	72.1	73.4	73.8	74.0	74.2	75.0	74.8	74.3	74.9	75.2	71.7	74.4	62.6	71.8	74.4	75.0	74.4	74.4	75.5	59.5	97.3	100.0				
30 *Amblyospora bracteata*	63.9	64.2	63.5	64.5	64.9	65.0	63.5	63.8	63.8	64.1	64.0	64.6	64.7	65.1	63.9	66.2	66.2	62.8	64.3	55.9	63.3	65.1	65.9	65.3	65.5	65.0	53.0	66.7	66.8	100.0			
31 Zelenkaia trichopterae (=iMS 1)	75.1	75.1	74.2	74.2	73.5	74.2	70.7	70.9	74.2	74.8	74.3	75.0	75.6	75.0	74.8	76.2	76.4	72.7	79.2	64.4	78.5	**90.2**	**89.3**	**88.8**	**88.8**	**84.6**	75.7	70.1	70.5	61.9	100.0		
32 Zelenkaia sp. (=iMS 2)	74.9	74.9	74.0	74.0	73.3	74.0	70.6	70.7	74.0	74.5	73.9	74.8	75.4	74.7	74.5	76.0	76.1	72.5	79.9	64.0	79.1	**90.6**	**90.0**	**89.5**	**89.5**	**85.1**	75.2	69.5	69.9	61.6	99.2	100.0	
33 *Amblyospora ferocious*	69.3	69.4	70.1	70.2	70.5	71.7	67.9	68.5	69.4	74.7	73.9	74.9	75.3	75.3	70.7	71.5	71.0	69.4	72.6	63.5	72.7	76.2	76.3	75.8	76.0	75.1	59.2	67.8	69.7	60.4	76.2	76.0	100.0

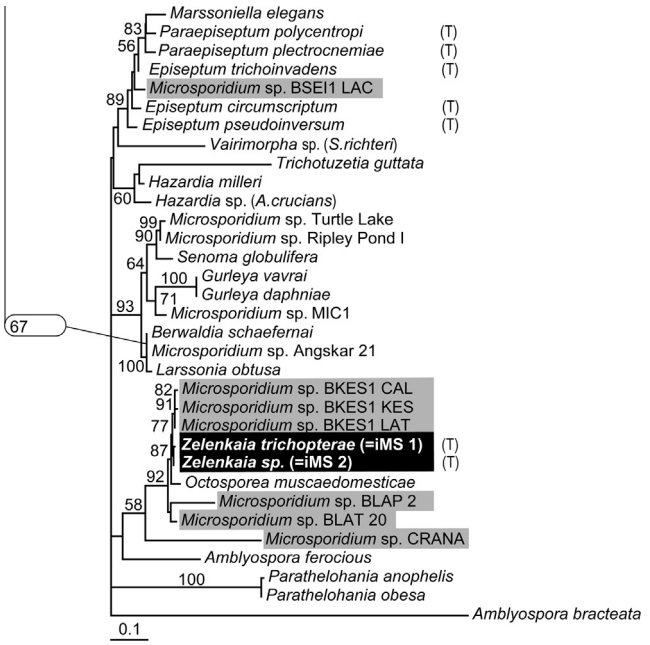

Fig. 37. Maximum Likelihood (ML) phylogenetic tree as inferred from partial SSU rRNA gene sequences. Microsporidia infecting amphipods (highlighted in grey) and caddisflies (T) group together in two diverse clades of the tree. Numbers above branches indicate ML bootstrap support (1000 replicates).

deletions). Percent nucleotide ssu rDNA sequence similarity between microsporidian species used in phylogenetic analysis is shown in Table 2.

SSU rDNA- and ITS-LSU-inferred phylogenetic trees constructed by different algorithms, revealed similar topology (ML SSU rDNA tree is shown Fig. 37, MP SSU rDNA – on Fig. S1, Supplementary materials; trees build by LogDet–paralinear distances method, and ITS-LSU-inferred trees are not shown). Analyses revealed that iMS1 and iMS2 represent a very closely related taxonomic unit, forming a separate branch in a cluster with undescribed microsporidia parasitizing amphipod hosts (*Microsporidium* sp. BKES1 CAL, *Microsporidium* sp. BKES1 KES, *Microsporidium* sp. BKES1 LAT) and with *Octosporea muscaedomesticae*. This cluster fell into the superclade of microsporida parasitizing predominantly aquatic hosts. It displayed identical topology in all trees, though the placement of the cluster on the trees varied depending on the analysis used (Figs. 37 and S1).

4. Discussion

4.1. Molecular phylogeny

Phylogenetic analyses revealed that there exist two distinct clades in which caddisfly microsporidia occur. In both clades several uncompletely characterized (molecular data only) microsporidia from amphipods occur. The first clade is composed of tetrasporoblastic trichopteran microsporida *Episeptum* spp. and *Paraepiseptum* spp., an undescribed *Microsporidium* sp. BSEI1 LAC from amphipods, and the microsporidium *Marsoniella elegans* infecting ovaries of copepodes. The second clade includes the described microsporidia iMS1 and iMS2, three undescribed microsporidia from amphipods, *Microsporidium* sp. BKES1 CAL, *Microsporidium* sp. BKES1 KES, and *Microsporidium* sp. BKES1 LAT (Figs. 37, and S1) and the dipteran microsporidian *Octosporea muscadomesticae.* According to rDNA-based phylogenetic analyses, *O. muscaedomesticae* is the species most closely related to the microsporidia iMS1 and iMS2 (75.7% similarity). This similarity, however, involves phylogeny data only, as *O. muscaedomesticae* differs from iMS1 and iMS2 in morphology, development, host specificity and tissue tropism. *O. muscaedomesticae* Flu, 1911 lives in the midgut epithelium of larval and adult house flies *Musca domestica* (Diptera, Muscidae) and other muscoid flies, is monomorphic throughout the life cycle, and is diplokaryotic with octosporoblastic sporogony in a subpersistent SPOV. Fresh spores average 5.4–7.3 × 1.8–2.4 μm (Kramer, 1964; Ormières et al., 1976). Although its host is a terrestrial insect, *O. muscaedomesticae* belongs to a clade containing microsporidian parasites of freshwater hosts (Vossbrinck et al., 2010).

4.2. Mutual relationship of iMS1 and iMS2

The extremely similar appearance of spores of both trichopteran microsporidian isolates, iMS1 and iMS2, suggests their close relationship or even identity. Close sister relationships were confirmed by high SSU rDNA sequence similarity (99.2% of similarity) and by SSU rDNA-inferred phylogenetic analyses by all method used.

4.3. iMS1 and iMS2 versus other microsporidia from Trichoptera

Twenty-four species of microsporidia, belonging to 10 genera, have been described from Trichoptera (the number in parentheses in the text below indicates the number of Trichoptera parasitizing species described in the respective genera). All described trichopteran microsporidia produce sporophorous vesicles (SPOV) during sporogony. Thus, one of the main characters to be considered in generic assignment of iMS1 and iMS are the number of spores per vesicle and the SPOV structure. The genus Chytridiopsis (1) has two types of sporogony. One type produces polysporoblastic thick-walled SPOVs with 8, 12 or 16 spores, respectively, second type of sporogony produces free spores in a parasitophorous vacuole believed by Canning and Vávra (2000), to possibly be a thin-walled SPOV. The genera *Tardivesicula* (1) and *Vavraia* (1) are polysporoblastic with 8 to 100 spores in SPOV. The genera *Amblyospora* (4), *Pegmatheca* (1) and *Thelohania* (3) are octosporoblastic. *Gurleya* (2), *Episeptum* (6) and *Paraepiseptum* (4) are tetrasporoblastic. Only the genus *Issia* (1) produces two spores per sporophorous vesicle. However, the iMS1 isolate cannot be included in this genus as *Issia* is diplokaryotic throughout its life cycle and spores within the SPOV are permanently glued together by a cementing material (Weiser, 1977; Canning and Vávra, 2000). Additional characters that distinguish the type species *Issia trichopterae* Weiser, 1946 from the two microsporidian isolates discussed here are the host (*Plectrocnemia geniculata*) and the morphology of the mature spores (pyriform, 3.5–4 × 2 μm). Thus iMS1 and iMS2 cannot be assigned to any of the known microsporidian genera parasitizing Trichoptera.

4.4. iMS1 and iMS2 and microsporidia forming doublets of spores

The above discussion shows that iMS1 and iMS2 cannot be identified with any microsporidian genus in which microsporidia from Trichoptera were described. The question arises if the characteristic formation of sporophorous vesicles with spore doublets cannot help in generic assignment of microsporidia described in this paper. Table 3 demonstrates, that iMS1 and iMS2 possess in this respect a unique complex of specific characters and that these microsporidia cannot be assigned to none of the existing spore doublets forming genera. The original tetrasporoblastic sporogony giving rise finaly to two individual sporophorous vesicles, each with a pair of connected sporoblasts and later with two spores arranged in parallel is original and warrants the proposition of a new microsporidian genus.

Table 3
Comparison of specific characters of microsporidian genera forming doublets of spores.

Genus	Type species	Host	Site of infection	Spore size (μm)	1	2	3	4	5	6	Additional distinguish characters
Abelspora	*A. portucalensis*	*Carcinus maenas* (Crustacea, Decapoda)	Hepatopancreas	3.1–3.2 × 1.2–1.4	5–6	1	1	1	No	Persistent	Development in xenomas
Berwaldia	*B. singularis*	*Daphnia pulex* (Crustacea, Cladocera)	Adipose tissue, ovary and hypodermis	5.5–6.5 × 3.0	15–18	1	1	–	Joined	Persistent	Disporoblastic sporogony but spores lie in individual blister-like two-layered SPOV
Gurleyides	*G. biformis*	*Ceriodaphnia reticulata* (Crustacea, Cladocera)	Fat body	?	?	2	?	2	Permanently joined	?	Second type of single spores has SPOV with foam-like appearance
Evlachovaia	*E. chironomi*	*Chironomus plumosus* (Insecta, Diptera)	?	?	?	2	1 and 2	1	No	?	
Holobispora	*H. thermocyclopis*	*Thermocyclops oithinoides* (Crustacea, Copepoda)	Connective tissue of the ovary	5.0–5.4 × 2.3–2.8	?	1	1	?	Permanently joined	?	
Issia	*I. trichopterae*	*Plectrocnemia geniculata* (Insecta, Trichoptera)	Fat body of larvae	3.5–4 × 2	?	2?	2 (and 1 ?)	1	Joined	?	Slightly pyriform spores
Neoperezia	*N. chironomi*	*Chironomus plumosus* (Insecta, Diptera)	Fat body of larvae	6.1 × 3.4	22–27	1	1	1	Permanently joined	Non-persistent	Two-layered SPOV
Norlevinea	*N. daphniae*	*Daphnia longispina* (Crustacea, Cladocera)	Oocytes in the ovary	5.5–6.0 × 2.7–3.0	8	1	1	2	Permanently joined	Non-persistent	
Senoma	*S. globulifera*	*Anopheles messeae* (Insecta, Diptera)	Gut epithelium of larvae and pupae	3.6 × 2.4	10–12	1	2	–	Permanently joined	–	Spores cemented by a large electron-dense globule; absence of SPOV
Telomyxa	*T. glugeiformis*	*Ephemera vulgata* (Insecta, Ephemeroptera)	Fat body of larvae	4.0 × 2.5	8–14	1	1	1	Permanently joined	Persistent	Rigid SPOV
Unikaryon	*U. pyriformis*	*non-specified trematode* (Platyhelminthes,Trematoda)	?	3.0 × 1.8[a]	6–6.5[a]	1	1	1	?	?	
Zelenkaia gen. n.	***Z. trichopterae n. sp. (=iMS 1)***	***Halesus digitatus* (Insecta, Trichoptera)**	**adipose tissue of larvae**	**9.6–11.2 × 3.3–3.7**	**24–26**	**1**	**1**	**1**	**No**	**non-persistent**	**Helical secretory material in immature SPOV**

Abbreviation used: 1 – number of polar filament coils, 2 – spores of one or two type, 3 – number of nuclei in the spore (2 = diplokaryon), 4 – number of doublets per SPOV, 5 – connection of spores, 6 – persistence of SPOV.
[a] Description based on *Unikaryon legeri* as no EM data on type sp. exists.

It can be concluded that the microsporidia iMS1 and iMS2 possess unique morphological, developmental and ultrastructural characteristics and form a single, distinct clade in phylogenetic trees based on rDNA analysis. This allows us to propose a new microsporidian genus for both the iMS1 and iMS2 with the type species represented by iMS1.

5. Taxonomic summary

5.1. Genus Zelenkaia n. gen.

5.1.1. Definition

Merogony: Uninucleate and binucleate (no diplokarya) meronts.

Sporogony: A plasmodium with four nuclei gives rise by rosette-like budding to two pairs of sporoblasts, first connected by their basal parts. A thinwalled sporophorous vesicle surrounds each sporoblasts pair. Spores uninucleate, two spores positioned in parallel as a non-cemented, yet associated pair within a non-persistent, thin-walled sporophorous vesicle.

5.2. Zelenkaia trichopterae n. sp.

5.2.1. Specific diagnosis

Fresh mature spores long oval, uninucleate, 10.3 × 3.5 μm (9.6–11.2 × 3.3–3.7 μm). Polar filament slightly anisofilar, forming 24–26 coils in a single row with two parts: anterior with 13–14 thin coils (120–140 nm), and posterior with 11–12, thicker (130–160 nm) coils. Polaroplast with two parts: anterior with regular, close packed lamellae and posterior with straight, less regular lamellae. The exospore (50 nm; 49–52 nm) composed of at least 10 distinct layers; endospore (180 nm; 160–180 nm). Immature sporophorous vesicle contains one large helical cluster of lamellar secretory material in the episporontal space.

Type host: *H. digitatus* (Schrank, 1781) (Trichoptera, Limnephilidae), larvae.

Type locality: Lower part of a small temporary foothill stream in the vicinity of village Levishte, Bulgaria (43°07′59.14″ North; 23°46′04.62″ East).

Site of infection: Adipose tissue.

Transmission: Unknown.

Interface: Merogonial stages in direct contact with host cell cytoplasm, sporogonial stages enclosed in a non-persistent sporophorous vesicle.

Etymology: The genus is named in honor of an outstanding Czech Baroque music composer Jan Dismas Zelenka (1679–1745).

Type material: Syntype slides, Giemsa stained smears of infected adipose tissue of *Halesus digitatus*, are deposited at the Smithsonian Institute, Washington, DC, USA, Accession No. USNM 1099766, in the type slide collection of Dr. Jaroslav Weiser, Faculty of Science, Charles University, Prague, Czech Republic and in the collection of the first author. The living spores of this isolate are preserved in the liquid nitrogen collection at Department of Parasitology, Faculty of Science, Charles University, Prague, Czech Republic.

Remarks: Partial nucleotide sequences, SSU, ITS and LSU rDNA, deposited in the NCBI GenBank, Accession Nos. EF537878, EF537879. Another, undescribed species, *Zelenkaia* sp., parasitizes larvae of *Micropterna sequax* McLachlan 1875, has spores of the same shape as in *Z. trichopterae*, measuring 9.5 × 3.7 μm (9.2–9.7 × 3.5–3.8 μm). Partial nucleotide sequences, SSU, ITS and LSU rDNA, are deposited in the NCBI GenBank, Accession Nos. EF537880, EF537881).

Acknowledgments

We extend our thanks to Dr. Leellen Solter (Illinois Natural History Survey and the University of Illinois at Urbana-Champaign, USA) for an invaluable help to improve this manuscript both as the scientific and editorial aspects are concerned, to Dr. Daniela Pilarska (Institute of Zoology, Bulgarian Academy of Sciences, Sofia, Bulgaria) for help with collecting of isolates, Dr. Jan Špaček (Labe River Authority, Hradec Králové, Czech Republic), Dr. Pavel Chvojka (Department of Entomology, Natural History Museum, Prague, Czech Republic) and Dr. Krassimir Kumanski (National Museum of Natural History, Bulgarian Academy of Sciences, Sofia, Bulgaria) for help with the identification of trichopteran hosts and Mrs. Eva Kirchmannová for help in electron microscopy. This work was supported by the following grants: MSMT 30-801 and FRVS 1789/2001 (both Czech Ministry of Education) and Z60220518 (Research Project of the Institute of Parasitology, Czech Academy of Sciences).

Appendix A. Supplementary material

Supplementary data associated with this article can be found, in the online version, at http://dx.doi.org/10.1016/j.jip.2013.04.010.

References

Andreadis, T.G., 2005. Evolutionary strategies and adaptations for survival between mosquito-parasitic microsporidia and their intermediate copepod hosts: a comparative examination of *Amblyospora connecticut* and *Hyalinocysta chapmani* (Microsporidia: Amblyosporidae). Folia Parasitol. 52 (1–2), 23–35.

Andreadis, T.G., Simakova, A.V., Vossbrinck, C.R., Shepard, J.J., Yurchenko, Y.A., 2012. Ultrastructural characterization and comparative phylogenetic analysis of new microsporidia from Siberian mosquitoes: evidence for coevolution and host switching. J. Invertebr. Pathol. 109, 59–75.

Becnel, J.J., White, S.E., Shapiro, A.M., 2005. Review of microsporidia–mosquito relationships: from the simple to the complex. Folia Parasitol. 52, 41–50.

Cali, A., Takvorian, P.M., 2011. Microsporidia. In: Margulis, Lynn (Ed.), Handbook of Protoctista, second ed. Jones and Bartlett, Boston.

Canning, E.U., Vávra, J., Phylum Microsporidia Balbiani, 1882, 2000. In: Lee, J.J., Leedale, G.F., Bradbury, P. (Eds.), The Illustrated Guide to the Protozoa, second ed., vol. 1. Society of Protozoologists, Kansas, Lawrence, pp. 39–126.

Felsenstein, J., 2001. PHYLIP, Phylogeny Inference Package, Department of Genetics, University of Washington, Seattle, Version 3.6a3.

Flu, P.C., 1911. Studie über die im Darm der Stubenfliege, *Musca domestica* vorkommenden protozoären Gebilde. Zentralbl. Baketeriol. Parasitenkd., Infektionskr. Hyg. Abt. I. Orig. 57, 522–537.

Guindon, S., Gascuel, O., 2003. A simple, fast, and accurate algorithm to estimate large phylogenies by maximum likelihood. Syst. Biol. 52 (5), 696–704.

Heilveil, J.S., Kohler, S.L., Solter, L.F., 2001. Studies on the life cycle and transmission of *Cougourdella* sp., a microsporidian parasite of *Glossosoma nigrior* (Trichoptera: Glossosomatidae). Great Lakes Entomol 34 (1), 9–15.

Hyliš, M., Weiser, J., Oborník, M., Vávra, J., 2005. DNA isolation from museum and type collection slides of microsporidia. J. Invertebr. Pathol. 88, 257–260.

Hyliš, M., Oborník, M., Nebesářová, J., Vávra, J., 2007. Aquatic tetrasporoblastic microsporidia from caddisflies (Insecta, Trichoptera): characterisation, phylogeny and taxonomic reevaluation of the genera *Episeptum* Larsson, 1986, *Pyrotheca* Hesse, 1935 and *Cougourdella* Hesse, 1935. Eur. J. Protistol. 43 (3), 205–224.

Kramer, J.J., 1964. The microsporidian *Octosporea muscaedomesticae* Flu, a parasite of calypterate muscoid flies in Illinois. J. Insect Pathol. 6, 331–342.

Larsson, J.I.R., 1995. A light microscopic and ultrastructural study of *Gurleya legeri* sensu Mackinnon (1911) – with establishment of the new species *Gurleya dorisae* n. sp. (Microspora, Gurleyidae). Acta Protozool. 34, 45–56.

Ormières, R., Baudoin, J., Brugerolle, G., Pralavorio, R., 1976. Ultrastructure de quelques stades de la microsporidie *Octosporea muscaedomesticae* Flu, parasite de *Ceratitis capitata* (Wiedemann) (Diptère, Trypetidae). J. Protozool. 23, 320–328.

Swofford, D.L., 2000. PAUP∗ Phylogenetic Analysis Using Parsimony (∗and Other Methods). Sinauer Associates, Sunderland, MA.

Thompson, J.D., Gibson, T.J., Plesniak, F., Jeanmougin, F., Higgins, D.G., 1997. The ClustalX windows interface: flexible strategies for multiple sequence alignment aided by quality analysis tools. Nucl. Acids Res. 24, 4876–4882.

Vávra, J., 1964a. Recording microsporidian spores. J. Insect Pathol. 6, 258–260.

Vávra, J., 1964b. A failure to produce an artificial infection in cladoceran Microsporidia. J. Protozool. 11 (Suppl.), 35–36.

Vávra, J., Larsson, J.I.R., 1994. *Berwaldia schaefernai* (Jirovec, 1937) comb.n. (Protozoa, Microsporida), fine structure, life cycle, and relationship to *Berwaldia singularis* Larsson, 1981. Eur. J. Protistol. 30 (1), 45–54.

Vávra, J., Maddox, J.V., 1976. Methods in microsporidiology. In: Bulla, I.A., Cheng, T.C. (Eds.), Comparative Pathobiology, vol. 1. Plenum Press New York, London, pp. 281–319.

Vávra, J., Hyliš, M., Oborník, M., Vossbrinck, C.R., 2005. Microsporidia in aquatic microcrustacea: the copepod microsporidium *Marssoniella elegans* Lemmermann, 1900 revisited. Folia Parasitol. 52 (1–2), 163–172.

Vossbrinck, C.R., Andreadis, T.G., Vávra, J., Becnel, J.J., 2004. Molecular phylogeny and evolution of mosquito parasitic microsporidia (Microsporidia: Amblyosporidae). J. Eukaryot. Microbiol. 51 (1), 88–95.

Vossbrinck, C.R., Baker, M.D., Andreadis, T.G., 2010. Phylogenetic position of *Octosporea muscaedomesticae* (Microsporidia) and its relationship to *Octosporea bayeri* based on small subunit rDNA analysis. J. Invertebr. Pathol. 105, 366–370.

Weiser, J., 1977. Contribution to the classification of microsporidia. Věstn. Česk. Spol. Zool. 41, 308–320.

Weiss, L.M., Vossbrinck, C.R., 1999. Molecular biology, molecular phylogeny, and molecular diagnostic approaches to the microsporidia. In: Wittner, M., Weiss, L.M. (Eds.), The Microsporidia and Microsporidiosis. AMS Press, Washington, DC, pp. 129–171.

Wolinska, J., Spaak, P., Koerner, H., Petrusek, A., Seda, J., Giessler, S., 2011. Transmission mode affects the population genetic structure of *Daphnia* parasites. J. Evol. Biol. 24 (2), 265–273.